

Experimental Evidence of Crystallization Pressure inside Porous Media

L. A. Rijniers, H. P. Huinink, L. Pel, and K. Kopinga

Department of Applied Physics, Eindhoven University of Technology, P.O. Box 513, 5600 MB Eindhoven, The Netherlands

(Received 27 September 2004; published 23 February 2005)

Crystallization pressure of salt in porous materials is one of the mechanisms that may induce serious damage, for example, weathering of buildings and monuments of cultural heritage. Since this pressure also causes the solubility of the salt inside a porous material to differ from the bulk solubility, it can be assessed experimentally by measuring the solubility inside the pores. We show that this is possible by NMR, and study Na_2CO_3 and Na_2SO_4 in a series of model porous materials. Using the solubility data the crystal-liquid surface energies are estimated as $\gamma = 0.09 \text{ N/m}$ for $\text{Na}_2\text{CO}_3 \cdot 10\text{H}_2\text{O}$ and $\gamma = 0.06 \text{ N/m}$ for $\text{Na}_2\text{SO}_4 \cdot 10\text{H}_2\text{O}$. For pore sizes below about 30 nm, the resulting pressure exceeds the tensile strength of typical building materials (3 MPa). No pressure is induced by the metastable $\text{Na}_2\text{SO}_4 \cdot 7\text{H}_2\text{O}$, which suggests for this crystal a value of γ close to zero.

DOI: 10.1103/PhysRevLett.94.075503

PACS numbers: 61.50.Ks, 05.70.-a, 64.70.Dv, 82.60.-s

The presence of salts is widely recognized as an important cause of damage to both modern built structures and monuments of cultural heritage [1]. Apart from this, salts also play an important role in the weathering of rock formations. These damage processes have been investigated for several decades, but the mechanisms that control the development of damage by crystal growth are poorly understood. Two major mechanisms are generally assumed to be responsible for salt damage: hydration pressure and crystallization pressure. Hydration pressure may result from the expansion of salt crystals during hydration. Recent experiments [2], however, raise a certain doubt of whether this mechanism actually occurs.

In this Letter, we will evaluate the mechanism of crystallization pressure. Although a thermodynamic framework has been developed to describe the equilibrium state of crystals under confinement, no one has been able to actually probe this pressure within the pores of a material. We will demonstrate for the first time that the solubility change which is directly related to the crystallization pressure can be determined experimentally from ^1H and ^{23}Na NMR measurements.

If a crystal is growing from a solution confined in a small space, such as a pore in a porous material, its surface tension γ will give rise to excess pressure p within the crystal. This mechanism is similar to that underlying the capillary pressure occurring at a liquid-vapor interface inside a pore. The situation is illustrated schematically in Fig. 1. θ denotes the contact angle between the crystal-liquid interface and the pore wall, which is usually larger than 90° . For cylindrical pores with radius r the excess pressure can be approximated by [3]

$$p = \frac{-2\gamma \cos\theta}{r}, \quad (1)$$

where the factor of 2 results from the cylindrical pore geometry. It is obvious that this pressure increases for decreasing pore sizes.

Recently, it has been shown [4] that an excess pressure p in a crystal shifts the solubility C of the crystal from the bulk solubility C_0 . If we rewrite Eq. (48) of Ref. [4] in terms of observable physical quantities, we obtain

$$p = nRT \left[\frac{1}{\nu_s^c} \ln\left(\frac{C}{C_0}\right) - \frac{\chi \nu_w^l}{\nu_w^c} (C - C_0) \right]. \quad (2)$$

Here n is the number of ions per unit salt, R the gas constant, T the absolute temperature, ν_s^c the molar volume of the salt in the crystal (m^3/mol), ν_w^l the molar volume of the water in the liquid (l/mol), and ν_w^c the molar volume of the water in the crystal (l/mol). The factor χ ($= 1000$) accounts for the fact that the concentration C is given in mol/l instead of in mol/m^3 . The ratio of ν_s^c and ν_w^c is a measure for the degree of hydration of the crystal. If the crystals are anhydrous, this equation transforms into the commonly known equation [5,6]:

$$p = \frac{nRT}{\nu_s^c} \ln\left(\frac{C}{C_0}\right). \quad (3)$$

One should note that, in contrast to Eq. (1), Eqs. (2) and (3) are not based on *a priori* assumptions about the geometry of the pore and the crystal-liquid interface.

Equation (2) shows that the solubility of a salt inside pores can be different from that in a bulk solution, and increases when the stress on the crystal is compressive.

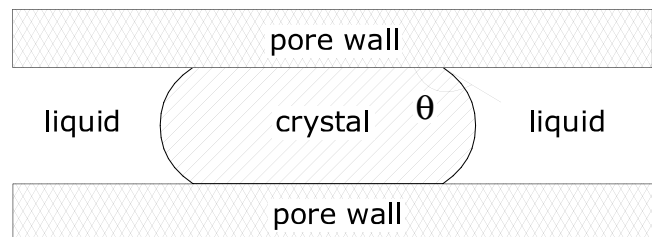


FIG. 1. Crystal confined in a cylindrical pore.

Hence the crystallization pressure can be assessed experimentally from the solubility increase inside the porous material. However, measurements of the solubility inside the pores, without disturbing it, are far from trivial. If this solubility is lower than the bulk value, it may be deduced from measurements in which a sample is immersed in a bulk solution. In this case, crystallization occurs within the pores of the material, which can be monitored by the concentration change of the bulk solution. However, when the solubility is higher than the bulk value, no information can be obtained with this technique, since crystallization occurs in the bulk. In this Letter, we will demonstrate that the solubility within the pores and the corresponding crystallization pressure can be determined directly from ^1H and ^{23}Na NMR measurements.

Usually salts have different crystal phases at different temperatures. As an example we consider Na_2SO_4 , which is one of the most damaging salts in porous building materials. It has two phases, mirabilite ($\text{Na}_2\text{SO}_4 \cdot 10\text{H}_2\text{O}$) and thenardite (anhydrous). The solubility for both phases is given in Fig. 2. The actual solubility is given by the lowest curve. From Eq. (2) it can be derived how the solubility changes if a pressure Δp is applied. This change is illustrated in Fig. 2. It appears that the transition from one phase to the other is shifted to lower temperatures.

The NMR apparatus used in this study operates at a magnetic field $B_0 = 0.78$ T, generated by an iron-cored electromagnet. The scanner is equipped with a Faraday shield to suppress the effect of changes of the sample properties [7]. The tuned circuit of the setup can be toggled between 33 MHz for H and 8.9 MHz for Na. The temperature of the sample holder can be accurately controlled by flowing a fluorinated cooling liquid, Galden®, through a heat exchanger in the wall of the sample holder. Since this

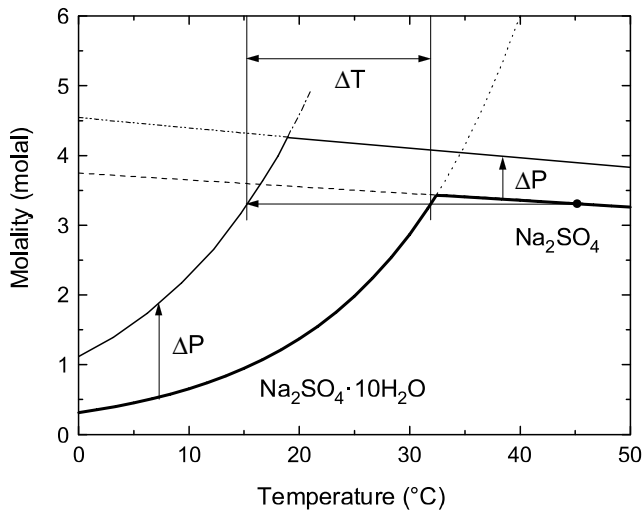


FIG. 2. An illustration of the change of the solubility and the temperature shift ΔT of the phase transformation of Na_2SO_4 when a pressure Δp is applied. The curves are calculated from Eq. (2).

fluid contains no H or Na, it yields no unwanted background signal in our NMR measurements.

To determine the relation between crystallization pressure and pore size, a model material with one dominant pore size is used. This material is a dried silica gel (Nucleosil®), which can be obtained in various pore sizes and various grain sizes. In our experiments all grain sizes were $10\ \mu\text{m}$. Each grain contains pores in the nanometer range. Nucleosil powder samples were prepared in a perspex cylinder of 18 mm inner diameter and height 3 mm. The powder was wetted with a solution of either Na_2SO_4 or Na_2CO_3 , saturated at $60\ ^\circ\text{C}$ and $40\ ^\circ\text{C}$, respectively. The wetting was continued just until the moment that excess bulk fluid could be observed. After wetting the samples the perspex holder was sealed using chloroform. At $40\ ^\circ\text{C}$ the concentration of the solution is known and can be used as a reference later on.

Next, the sample was placed in the NMR scanner and cooled to $2\ ^\circ\text{C}$. After nucleation had occurred the samples were heated slowly, such that thermodynamic equilibrium was always guaranteed, and during this heating NMR measurements were performed. Both Na and H intensity profiles and NMR relaxation times were measured. Because of the NMR echo time used in the experiments ($800\ \mu\text{s}$), only the Na nuclei in the solution are measured; no signal is observed from the crystals. For the same reason, the H nuclei of crystal water are not observed. From the intensity profiles the solution concentration can be determined. The relaxation measurements give information on the pore size [8]. The latter measurements can therefore be used to see whether damage has been induced in the sample. To calibrate the NMR signal, a 3 m NaCl reference sample is measured during every experiment. The solubility of NaCl is nearly constant in the range $0\ ^\circ\text{C}$ – $40\ ^\circ\text{C}$. Tests revealed that for bulk solutions our concentration measurements are accurate within 5%.

First, experiments were performed on Na_2CO_3 bulk solutions, and on solutions in pore sizes of 30, 10, and 7 nm. The pore sizes of these Nucleosils were checked by various techniques, such as N_2 adsorption, mercury intrusion porosimetry, and NMR relaxometry [9,10], and were found to agree fairly well with the nominal values specified by the manufacturer. These measurements also confirmed the monomodal pore-size distribution of these materials. The measured concentration for the bulk coincides with the solubility data from literature [11]. At $32\ ^\circ\text{C}$ a phase transition occurs between a decahydrated phase at lower temperatures and a monohydrated phase at higher temperatures. For the solution inside the pores, the measurements indicate a large temperature shift of this phase transition, which already shows the presence of a crystallization pressure. However, the measured concentration inside the pores was significantly lower than the expected value, even at $40\ ^\circ\text{C}$, where the concentrations within the bulk and the pores must be the same. This can be explained by the

quadrupolar character of the Na nucleus [12]. Under certain conditions, for instance, if surface charges are present at the pore wall, this may enhance the relaxation rate, resulting in a significant loss of Na signal before observation. This was verified by analyzing the relaxation behavior of several samples in a 11.7 T Bruker spectrometer. To correct for this effect a calibration was performed using a 100 nm Nucleosil sample. This sample did not show a temperature shift of the phase transition, and therefore its concentration in the entire temperature region is equal to the bulk solubility. This calibration was applied to all other samples. The resulting solubility measurements are given in Fig. 3.

It can be seen that the solubility inside the 30 nm pores hardly differs from the bulk solubility. However, the solubility inside the 7 and 10 nm pores is significantly higher. The solubility increase for the 7 nm pore amounts to a factor of 3.1 at 10 °C, whereas this factor is 2.3 for the nominal 10 nm pores. If we insert these factors in Eq. (2), we obtain crystallization pressures of 9 and 13 MPa for the 10 and 7 nm pores, respectively. Assuming cylindrical pores and a contact angle of 180° for the crystal-liquid interface, and a bulk water value $\gamma = 0.072$ N/m [11], it is possible to estimate the surface tension as $\gamma = (0.09 \pm 0.02)$ N/m. The error reflects the maximum experimental error in the solubility increase (about 3 standard deviations).

In contrast to the measurements on Na_2CO_3 , the measurements on Na_2SO_4 did not reveal any loss of Na signal. Na_2SO_4 has three possible crystal phases: an anhydrous phase (thenardite), a decahydrated phase (mirabilite), and a metastable heptahydrated phase [13]. The measured solu-

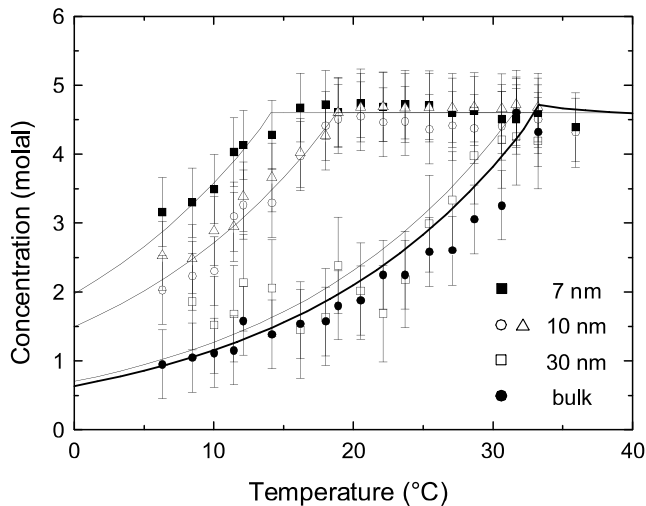


FIG. 3. Solubility of Na_2CO_3 in bulk and inside the pores of various Nucleosils. The curves reflect the bulk literature values or a description of the data by Eq. (2). For the 10 nm pores, measurements were performed on two different Nucleosil samples.

bilities of Na_2SO_4 of bulk solution and solutions in Nucleosil with pore sizes of 7, 10, and 30 nm are plotted in Fig. 4.

Almost all data coincide with the solubility of the $\text{Na}_2\text{SO}_4 \cdot 7\text{H}_2\text{O}$ crystal known from literature. Because this phase is metastable, it is expected to transform into $\text{Na}_2\text{SO}_4 \cdot 10\text{H}_2\text{O}$, but this was not observed. The solubility of the heptahydrated phase is independent of the pore size, which implies that the surface tension of this phase is very small. Hence no crystallization pressure occurs, and no damage will be induced. This was supported by an experiment with four temperature cycles. An analysis of the relaxation time distributions revealed no changes in the pore-size distributions. Only in one experiment on a 7 nm Nucleosil sample did we observe a solubility curve resembling that reported for $\text{Na}_2\text{SO}_4 \cdot 10\text{H}_2\text{O}$. The corresponding data are represented by the triangles in Fig. 4. In this experiment the solubility increase compared to the bulk was about a factor of 2 at 5 °C. This increase demonstrates that for the decahydrated crystal phase a crystallization pressure is present. This pressure amounts to about 8 MPa in the 7 nm pores. The surface tension of this phase can be estimated as $\gamma = (0.06 \pm 0.02)$ N/m. Again the error reflects the maximum experimental error in the solubility increase.

Our experiments demonstrate that by means of NMR the solubility of various salts inside porous materials can be observed directly. The measurements reveal that a crystallization pressure may exist inside porous materials, as was predicted theoretically. For Na_2CO_3 a significant solubility

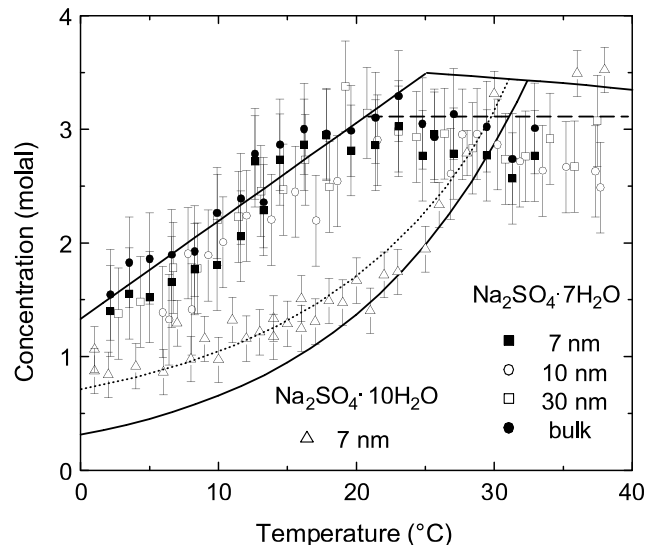


FIG. 4. Measured solubility of Na_2SO_4 in bulk and inside the pores of various Nucleosils. The horizontal dashed line represents the solubility at 60 °C. Solid lines and curves reflect bulk solubilities. The dotted curve through the data indicating the presence of $\text{Na}_2\text{SO}_4 \cdot 10\text{H}_2\text{O}$ in the 7 nm pores is meant only as a guide to the eye.

increase is observed in pores of 7 and 10 nm. Within experimental error, the resulting excess pressures satisfy the qualitative $1/r$ behavior given by Eq. (1), and can be expressed as $P = 0.045 \text{ (Nm}^{-1}\text{)}/r$. Assuming a typical tensile strength of 3 MPa of a building material [14], the typical pore size below which the crystallization pressure may cause damage is about 30 nm. For Na_2SO_4 a metastable phase is observed, which has no excess pressure and, consequently, will not cause any damage. Although this phase has been reported a long time ago [15], this has not always been appreciated in more recent studies, which implicitly assume a decahydrated phase [4,6]. The actual pressure caused by a $\text{Na}_2\text{SO}_4 \cdot 10\text{H}_2\text{O}$ crystal inside a pore with radius r can be estimated as $P = 0.03 \text{ (Nm}^{-1}\text{)}/r$, which implies that damage may be caused in pores with a typical size below about 20 nm.

In systems with multiple pore sizes, crystals will preferably grow in the largest pores if the crystallization pressure is positive. Hence the largest pore without a crystal determines the solubility increase. If the material is not fully saturated, the liquid-vapor interface may be located inside the pores. In this case, the surface tension of that interface may reduce the crystallization pressure [16].

It is evident that for porous materials with small pore sizes crystallization pressure is a damaging effect. From practice it is known, however, that also in materials having larger pores salt damage does occur. Probably this is caused by nonequilibrium effects, which are not considered in the present study. Experiments in which crystallization is not induced by lowering the temperature but by evaporation of water may be necessary to identify the exact mechanism causing these damages.

Part of this research was supported by the Dutch Technology Foundation (STW), the Priority Program Materials Research (PPM), and the Center for Building and Systems TNO-TUE.

-
- [1] A. Goudie and H. Viles, *Salt Weathering Hazards* (John Wiley and Sons, New York, 1997).
 - [2] C. Rodrigues-Navarro and E. Doehne, *Earth Surf. Processes Landforms* **24**, 191 (1999).
 - [3] A. Adamson, *Physical Chemistry of Surfaces* (Wiley Interscience, Chichester, 1960).
 - [4] R. Flatt, *J. Cryst. Growth* **242**, 435 (2002).
 - [5] C. W. Correns, *Discuss. Faraday Soc.* **5**, 267 (1949).
 - [6] G. W. Scherer, *Cem. Concr. Res.* **29**, 1347 (1999).
 - [7] K. Kopinga and L. Pel, *Rev. Sci. Instrum.* **65**, 3673 (1994).
 - [8] K. R. Brownstein and C. E. Tarr, *Phys. Rev. A* **19**, 2446 (1979).
 - [9] L. Rijniers, P. Magusin, H. Huinink, L. Pel, and K. Kopinga, *J. Magn. Reson.* **167**, 25 (2004).
 - [10] R. Valckenborg, L. Pel, and K. Kopinga, *J. Phys. D* **35**, 249 (2002).
 - [11] D. Lide, *CRC Handbook of Chemistry and Physics* (CRC Press LLC, Boca Raton, FL, 1998).
 - [12] P. Porion, M. Al Mukhtar, S. Meyer, A. Faugere, J. van der Maarel, and A. Delville, *J. Phys. Chem. B* **105**, 10505 (2001).
 - [13] O. Braitsch, *Salt Deposits, Their Origin and Composition* (Springer, New York, 1971).
 - [14] A. Vermeltfoort, *Masonry International* **10**, 85 (1997).
 - [15] *Gmelins Handbuch der anorganische Chemie*, edited by R. Meyer (Verlag Chemie GMBH, Weinheim, 1928).
 - [16] L. Rijniers, Ph.D. thesis, Eindhoven University of Technology, 2004.